Int. J. Heat Mass Transfer. Vol. 36, No. 1, pp. 147–153, 1993
Printed in Great Britain

0017–9310/93 $5.00 + 0.00

Roughness element shape effects on heat transfer and skin friction in rough-wall turbulent boundary layers

M. H. HOSNI
Department of Mechanical Engineering, Kansas State University, Manhattan, KS 66506, U.S.A.

HUGH W. COLEMAN
Mechanical Engineering Department, University of Alabama in Huntsville, Huntsville, AL 35899, U.S.A.

and

JAMES W. GARNER and ROBERT P. TAYLOR
Thermal & Fluid Dynamics Laboratory, Mechanical and Nuclear Engineering Department, Mississippi State University, Mississippi State, MS 39762, U.S.A.

(*Received* 26 *June* 1991 *and in final form* 20 *February* 1992)

Abstract—Stanton number and skin friction coefficient results are presented for zero pressure gradient incompressible turbulent boundary layer air flows over two rough surfaces composed of 1.27 mm base diameter by 0.635 mm high truncated cones spaced in staggered arrays two ($L/d_0 = 2$) and four diameters ($L/d_0 = 4$) apart, respectively, on otherwise smooth walls. These data are compared with previously reported results obtained in the same test facility under similar flow conditions using equivalently sized and spaced hemisphere roughened surfaces. It is shown that the Stanton number data (which have uncertainties of about 2–4%) exhibit slightly distinguishable differences for the two $L/d_0 = 4$ surfaces and definitive differences for the two $L/d_0 = 2$ surfaces. No dependence of skin friction coefficients on roughness element shape could be concluded considering the uncertainty in the data. Predictions of Stanton number and skin friction coefficient distributions from the finite difference solutions of discrete element equations are presented and compared with the experiments.

INTRODUCTION

HEAT TRANSFER and skin friction for turbulent flow over a particular surface are of primary interest in the design and analysis of engineering systems. Most heat transfer experimental efforts to date have focused on boundary layer flow over smooth surfaces, resulting in extensive heat transfer and fluid dynamics data sets which apply fundamentally to smooth surfaces. Many engineering designs involve surfaces that, in the aerodynamic sense, are rough rather than smooth; thus, a practical need is established for comprehensive data sets for turbulent flow over well-defined rough surfaces. Turbine blades, impellers, ship and submarine hulls, high performance aircraft, heat exchangers, and piping systems are typical instances where surface roughness can significantly influence heat transfer and fluid dynamic characteristics. In order to properly and efficiently design such systems, an accurate predictive model for the behavior of turbulent flow over rough surfaces is needed. To develop such a model, accurate, precise, well-posed experimental data sets for turbulent flow over surfaces with well-defined surface roughness are required.

The work reported in this article extends our previously reported results [1, 2] by considering roughness element shape effects on rough-wall turbulent boundary layer flow and heat transfer through direct comparison of heat transfer and fluid dynamics data sets obtained in the same facility using rough surfaces with different roughness geometries. Stanton number and skin friction coefficient results are presented for zero pressure gradient, constant wall temperature, incompressible turbulent boundary layers over two surfaces roughened with 1.27 mm base diameter by 0.635 mm high truncated cones spaced in staggered arrays two and four base diameters apart, respectively, on otherwise smooth walls. These data are compared directly with data from the previously reported [1, 2] experiments in the same facility that used two surfaces roughened with hemispheres with the same height, base diameter, and spacing as the truncated cones. The roughness element shapes and layout are shown schematically in Fig. 1. The test surfaces differ in the shape, surface area, and projected frontal area of the roughness elements. The projected frontal area ratio of hemispheres to truncated cones is 1.35, and the surface area ratio is 1.32.

In addition, predictions of Stanton number distributions and skin friction coefficient distributions

NOMENCLATURE

C_D	roughness element drag coefficient
C_f	skin friction coefficient, $2\tau_w/\rho U_\infty^2$
C_p	specific heat
d_0	roughness element base diameter
$d(y)$	local roughness element diameter
H	enthalpy
k	roughness element height
k'	projected height for truncated cones
K	roughness element thermal conductivity
L	spacing of roughness elements
Nu_d	roughness element Nusselt number
p	pressure
Pr	Prandtl number
Re_d	Reynolds number based on local roughness element diameter
Re_x	x-Reynolds number, $\rho U_\infty x/\mu$
Re_{δ_2}	momentum thickness Reynolds number, $\rho U_\infty \delta_2/\mu$
St	Stanton number
T	local fluid static temperature
T_R	roughness element temperature
u	mean longitudinal velocity
$\overline{u'v'}$	Reynolds shear stress factor
U_∞	freestream velocity
v	mean normal velocity
$\overline{v'h'}$	turbulent heat flux factor
x	axial distance from nozzle exit
y	coordinate normal to surface.

Greek symbols

β_x	blockage factor
β_y	blockage factor
δ_2	momentum thickness
μ	dynamic viscosity
ν	kinematic viscosity
ρ	density.

Subscripts

W	wall
∞	freestream.

from the finite difference solution of discrete element equations are compared with the data. These predictions used exactly the same roughness models as previously reported [1, 2] in the investigation which used the hemispherical roughness elements.

In the article [1] reporting the results for the surfaces roughened with hemispherical elements, an extensive discussion of previous experimental and computational efforts in roughness influenced flows was presented and will not be repeated here. The data for the surfaces with truncated cone roughness elements were obtained in the Turbulent Heat Transfer Test Facility (THTTF), shown schematically in Fig. 2, using exactly the same equipment and procedures as for the previously reported results. The facility and procedures were discussed in great detail in ref. [1]. The facility and computations are only summarized here.

Description of Surface Roughness Elements

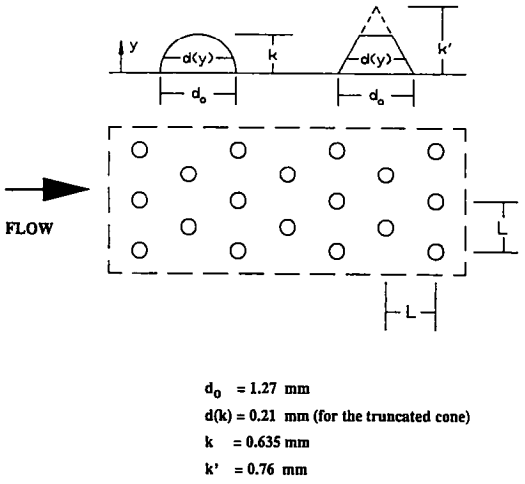

FIG. 1. Description of surface roughness shape and nomenclature for the truncated cone and hemisphere roughened surfaces.

COMPUTATION

The steady (Reynolds-averaged), two-dimensional turbulent boundary layer equations presented here are for flow over a rough surface with roughness elements of uniform shape and spacing as derived by Taylor *et al.* [3, 4]. The equations are:

$$\frac{\partial}{\partial x}(\rho\beta_x u)+\frac{\partial}{\partial y}(\rho\beta_y v)=0 \tag{1}$$

$$\beta_x\rho u\frac{\partial u}{\partial x}+\beta_y\rho v\frac{\partial u}{\partial y}=-\frac{\partial}{\partial x}(\beta_x p)+\frac{\partial}{\partial y}\left[\beta_y\left(\mu\frac{\partial u}{\partial y}-\overline{\rho u'v'}\right)\right]-\tfrac{1}{2}\rho C_D d(y)\frac{u^2}{L^2} \tag{2}$$

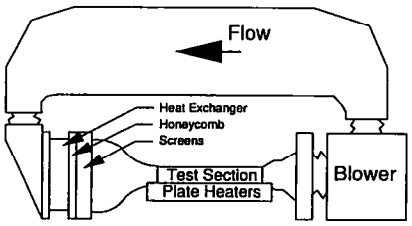

FIG. 2. Schematic of the Turbulent Heat Transfer Test Facility (THTTF).

$$\beta_x \rho u \frac{\partial H}{\partial x} + \beta_y \rho v \frac{\partial H}{\partial y} = \frac{\partial}{\partial y}\left[\beta_y \left(\frac{K}{C_p}\frac{\partial H}{\partial y} - \overline{\rho v' h'}\right)\right] + u\frac{\partial}{\partial x}(\beta_x p) + \beta_y \frac{\partial u}{\partial y}\left[\mu \frac{\partial u}{\partial y} - \overline{\rho u' v'}\right] + \tfrac{1}{2}\rho C_D \frac{d(y)}{L^2} u^3 + \pi \frac{K Nu_d}{L^2}(T_R - T). \quad (3)$$

Examination of equations (2) and (3) shows that empirical models for $-\overline{\rho u' v'}$, $-\overline{\rho v' h'}$, the roughness element drag coefficient, $C_D(y)$, and the roughness element Nusselt number, $Nu_d(y)$, are necessary for closure. The blockage parameters, β_x and β_y, and the element shape descriptor, $d(y)$, require no empirical fluid mechanics input as they are determined solely from the geometry of the rough surface.

The roughness element $C_D(y)$ and $Nu_d(y)$ models are formulated as functions of the local element Reynolds number $Re_d = u(y)d(y)/\nu$ which includes roughness element size and shape information through $d(y)$. As discussed in Taylor *et al.* [3], the $C_D(y)$ model which gave the best overall agreement was

$$\log C_D = -0.125 \log (Re_d) + 0.375. \quad (4)$$

This model has been tested for values of Re_d up to 25 000 [3, 5] using many data sets and was used unchanged for the predictions presented in this work.

The roughness element energy transport model requires empirical input in the form of a Nusselt number, $Nu_d(d)$. Hosni *et al.* [2] developed the model

$$Nu_d = 1.7 Re_d^{0.49} Pr^{0.4} \quad (5)$$

which was used unchanged in this work. This model has been tested up to Re_d of about 2200.

The turbulence closure models used were a Prandtl mixing length with Van Driest damping and a constant turbulent Prandtl number. These models and the numerical solution procedure for the discrete element equations are discussed in detail elsewhere [2].

EXPERIMENTAL APPARATUS AND MEASUREMENT PROCEDURES

The experiments were performed in the THTTF which is shown in Fig. 2. Complete descriptions of the facility and its qualification are presented in Hosni *et al.* [1]. This facility is a closed loop wind tunnel with a freestream velocity range of 6–67 m s^{-1}. The temperature of the circulating air is controlled with an air to water heat exchanger and a cooling water loop. Following the heat exchanger the air flow is conditioned by a system of honeycomb and screens.

The bottom wall of the nominally 2.4 m long by 0.5 m wide by 0.1 m high test section consists of 24 electrically heated flat plates which are abutted together to form a continuous flat surface. Each nickel plated aluminum plate (about 10 mm thick by 0.1 m in the flow direction) is uniformly heated from below by a custom-manufactured rubber-encased electric heater pad. Design computations showed that, with this configuration, a plate can be considered to be at a uniform temperature. The precision machined rough test surfaces considered here have 1.27 mm base diameter by 0.635 mm high truncated cone elements spaced two and four diameters apart in staggered arrays as shown in Fig. 1. The measured average surface roughness on the 'smooth' wall portion of the plates is less than 1.6 μm, and the allowable step (or mismatch) between any two plates is 0.013 mm. The heating system is under active computer control and any desired set of plate temperatures can be maintained within the limits of the power supply. To minimize the conductio ı losses, the side rails which support the plates are heated to approximately the same temperature as the plates.

The top wall can be adjusted to maintain a constant freestream velocity along the length of the test section. An inclined water manometer with resolution of 0.06 mm is used to measure the pressure gradient during top wall adjustment. Static pressure taps are located in the side wall adjacent to each plate. The pressure tap located at the second plate is used as a reference, and the pressure difference between it and each other tap is minimized. For example, the maximum pressure difference for the 43 m s^{-1} case was 0.3 mm of water.

The boundary layer is tripped at the exit of the 19 : 1 area ratio nozzle with a 1 mm × 12 mm wooden strip. This trip location is immediately in front of the heated surface.

For the THTTF Stanton number data in this paper, the overall uncertainty, as discussed in detail by Hosni *et al.* [2], ranged from about ±2% to ±5%, depending on flow conditions.

DISCUSSION

Experimental Stanton number and skin friction coefficient distributions are presented for turbulent boundary layer flows over two rough surfaces with truncated cone roughness elements. These data are compared directly with the previously reported data from two rough surfaces with hemispherical roughness elements of the same roughness height, base diameter and spacings which were obtained under equivalent flow conditions using the same experimental facility and measurement procedures. Calculations of Stanton number and skin friction coefficient distributions using the discrete element prediction method are also compared with the data.

Experimental results

The Stanton number data are presented graphically in St vs Re_x coordinates. Values of Re_x were computed with length scale (x) taken as the distance from the leading edge of the first test plate. In order to contrast the data for rough surfaces with the smooth wall results, the smooth wall Stanton number correlation expression [6]

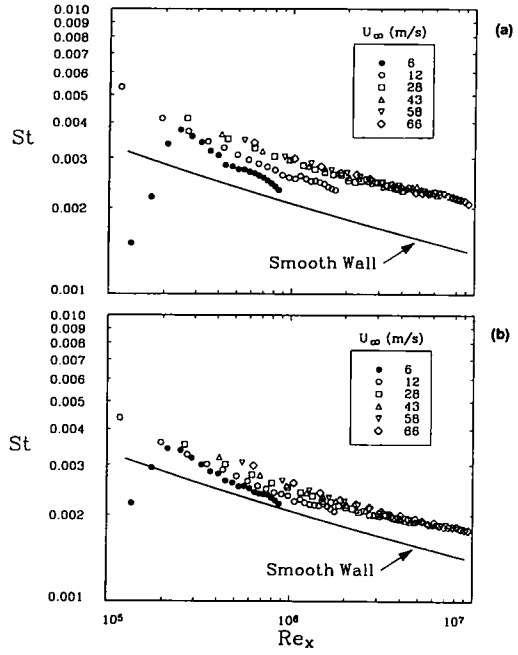

FIG. 3. Composite plot of the Stanton number data vs Re_x for surfaces with truncated cone roughnesses: (a) $L/d_0 = 2$; (b) $L/d_0 = 4$.

$$St = 0.185[\log_{10}(Re_x)]^{-2.584}\, Pr^{-0.4} \qquad (6)$$

is used.

Figures 3 and 4 show composite plots of the Stanton number data for both the truncated cone and hemisphere roughness surfaces. These figures clearly show the increase in Stanton number with increased roughness density. For the truncated cone roughened surface with $L/d_0 = 2$, the increase in St over the equivalent smooth wall case is about 55%; and for $L/d_0 = 4$, the increase is about 30%. For the companion hemisphere roughened surface with $L/d_0 = 2$, the increase in St over the equivalent smooth wall case is about 75%; and for $L/d_0 = 4$, the increase is about 40%.

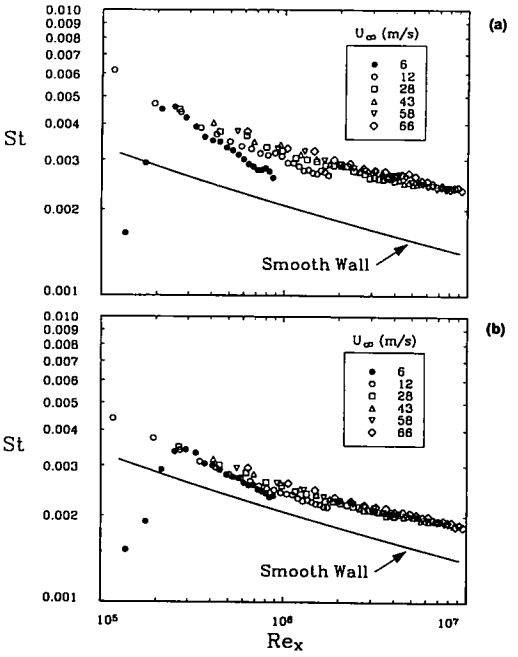

FIG. 4. Composite plot of the Stanton number data vs Re_x for surfaces with hemisphere roughnesses: (a) $L/d_0 = 2$; (b) $L/D_0 = 4$.

As discussed in ref. [1], smooth-wall data sets corresponding to different freestream velocities collapse to a single curve in these coordinates. For these rough surfaces, the Stanton number data sets appear to collapse to single, asymptotic curves for $U_\infty = 28$ m s^{-1} and greater. However, the Stanton numbers at $U_\infty = 6$ and 12 m s^{-1} exhibit a distinct shift from the corresponding data sets taken at higher freestream velocities. This behavior can be discussed using the concepts of fully-rough and transitionally-rough flows, the definitions of which are based only on fluid mechanics considerations. As the freestream velocity increases, the turbulent flow over a rough surface evolves from aerodynamically smooth to transitionally rough and finally to a new asymptotic state—fully rough. Based on the work of Hosni *et al.* [1, 2], Garner *et al.* [7] classify the $U_\infty = 6$ and 12 m s^{-1} flows as transitionally rough and the other velocities as fully rough from a fluid mechanics viewpoint for the $L/d_0 = 4$ truncated cone surface. For the $L/d_0 = 2$ truncated cone surface, these classifications are transitionally rough for $U_\infty = 6$ m s^{-1} and fully rough for the $U_\infty \geqslant 12$ m s^{-1} cases. Apparently, the thermal and fluid mechanics asymptotic rough flow conditions are not exactly the same, since the $U_\infty = 12$ m s^{-1}, $L/d_0 = 2$ surface has clearly not reached the thermal asymptotic state.

Figure 5 is a composite data plot which compares directly the Stanton number results for the truncated cone roughened surfaces and the corresponding hemisphere roughened surfaces for matched flow conditions. There is a clear difference in the Stanton number data for the hemisphere roughened surface and the truncated cone roughened surface with the same height, spacing and aspect ratio. Typically, the Stanton number data are about 10% higher for the $L/d_0 = 2$ surfaces and 2–4% for the $L/d_0 = 4$ surfaces roughened with hemispheres compared with equivalent surfaces roughened with truncated cones. As perhaps should be expected, the effect of the shape on the heat transfer is a function of the element spacing, with the larger effect at the more dense spacing. Also, there appears to be some indication of a freestream velocity influence on the difference. As seen in Table 1 the ratio of hemisphere Stanton number to cone Stanton number is on average slightly larger for the lower velocities. This perhaps indicates a different rate of evolution toward the thermal asymptotic state discussed above.

This apparent effect of the roughnes element shape difference on Stanton number is believed to be real and physically meaningful, even though the observed

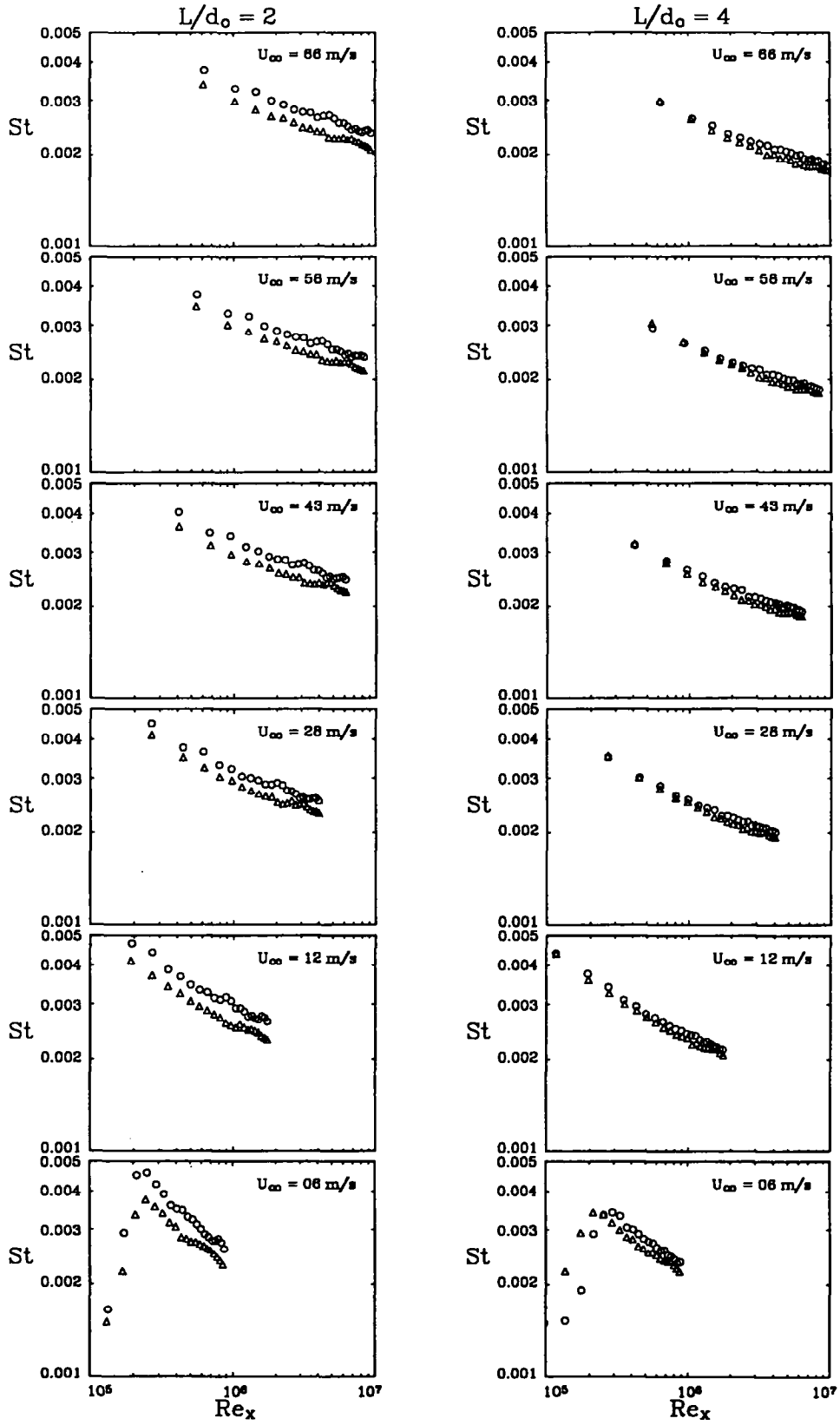

FIG. 5. Composite plot of the Stanton number data vs Re_x for $U_\infty = 6$, 12, 28, 43, 58 and 66 m s^{-1} for the $L/d_0 = 2$ and 4 surfaces (hemisphere, circle; truncated cone, triangle).

Table 1. Comparison of Stanton number ratios

	St_H/St_C	
U_∞ (m s^{-1})	$L/d_0 = 4$	$L/d_0 = 2$
6	1.07	1.14
12	1.04	1.14
28	1.04	1.09
43	1.05	1.10
58	1.04	1.10
66	1.05	1.12

difference is marginally the same as the uncertainty in Stanton number (2–4%) for the $L/d_0 = 4$ cones. The experimental apparatus and measurement procedures used to obtain these Stanton numbers were the same; thus the bias errors are highly correlated for both test surfaces. Garner *et al.* [7] demonstrated excellent repeatability of the Stanton number distributions for a given freestream velocity.

Figure 6 shows comparisons of skin friction coefficient distributions for the truncated cone surfaces with the comparable hemisphere surfaces for freestream velocities of 12 and 58 m s^{-1} plotted versus the momentum thickness Reynolds number. The solid and dashed lines are predictions, which are discussed later. This figure shows that skin friction coefficients for both THTTF roughness shapes for both the $L/d_0 = 2$ and 4 surfaces are the same within the indicated uncertainty bounds (10%) associated with the hot-wire measurement technique. Scaggs *et al.* [5] also found no difference in friction factor for cones and hemispheres in their pipe flow experiments. The smooth wall line shown for comparison is the turbulent flat plate boundary layer correlation from Kays and Crawford [8]

$$\frac{C_f}{2} = 0.0125(Re_{\delta_2})^{-0.25}. \quad (7)$$

Profiles of mean temperature, mean velocity and the three Reynolds normal stress components were also compared. For matched flow conditions, no effect of roughness element shape could be concluded when the uncertainty of the data was considered.

Predictions

Figure 7 shows a comparison of data and predictions for both the hemisphere and truncated cone surfaces for a freestream velocity of 12 m s^{-1}. The boundary layer predictions using the discrete element method are 'true' predictions for the truncated cone cases in that no information from those experiments were used in the calculations. The model is based on the hemisphere data of Hosni *et al.* [1] and was used unchanged for the current predictions. The figure shows that the agreement is excellent for the $L/d_0 = 4$ cases. However, the model slightly overpredicts the truncated cone data for the $L/d_0 = 2$ surface. The predictions are about 2–12% higher than the data, but the trend of the data is accurately predicted. The 'wiggles' in the predictions are a result of the solution procedure. As the boundary layer grows, the computational grid expands to fill the boundary layer in the physical domain, and periodically the number of grid points below the crest of the elements decrease by one. Results for freestream velocities of 43 and 66 m s^{-1} show similar trends.

Considering the effects of surface roughness shape on the discrete element predictions of Stanton number, the model seems to correctly predict the difference for the $L/d_0 = 4$ cases, but it does not show as large an effect of shape at $L/d_0 = 2$ as the data indicate. Even so, the predictions of these cases are within about 10%.

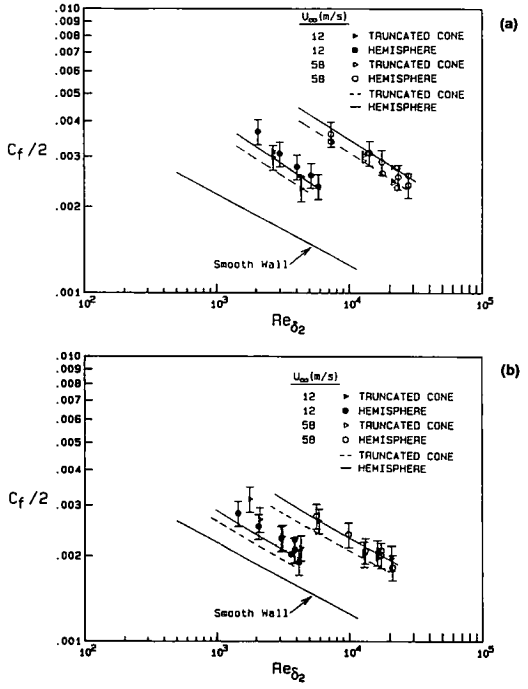

FIG. 6. Comparison of skin friction coefficient data and predictions vs momentum thickness Reynolds number: (a) $L/d_0 = 2$; $L/d_0 = 4$.

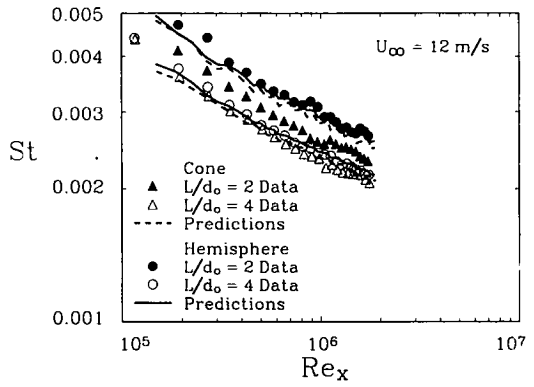

FIG. 7. Comparisons of the Stanton number data and predictions for both the hemisphere and truncated cone surfaces for freestream velocity of 12 m s^{-1}.

Referring back to Fig. 6, skin friction coefficient data for the $L/d_0 = 2$ and 4 surfaces with truncated cone and hemisphere roughness are compared with C_f calculations made using the discrete element prediction scheme for freestream velocities of 12 and 58 m s^{-1}. Comparisons of skin friction coefficient data and predictions show that the predictions exhibit a behavior that is typical of the data. For the freestream velocity of 58 m s^{-1}, predictions and data agree within the data uncertainty. For a freestream velocity of 12 m s^{-1}, the data and predictions for the hemisphere roughness agree within the data uncertainty for both $L/d_0 = 2$ and 4, but predictions for the truncated cone roughness fall slightly below the uncertainty bands of the data.

SUMMARY AND CONCLUSIONS

The Stanton number data, which have uncertainties of about 2–4%, exhibit slightly distinguishable differences for the two $L/d_0 = 4$ surfaces and definitive differences for the two $L/d_0 = 2$ surfaces. In St vs Re_x coordinates, for $L/d_0 = 4$ the Stanton numbers are consistently about 2–4% larger for the surface with hemispherical roughness than for the surface with conical roughness. For $L/d_0 = 2$, this difference is increased to about 10–12%. No dependence of skin friction coefficients on roughness element shape could be concluded considering the uncertainty of the hot-wire anemometry technique, which was used to determine C_f.

Predictions of Stanton number distributions from the finite difference solution of discrete element equations are in excellent agreement with the data from the surface with truncated cone roughness at $L/d_0 = 4$ and are about 2–12% high for the $L/d_0 = 2$ cases. Skin friction coefficient data and predictions also agree within the data uncertainty with the exception of the 12 m s^{-1} case where predicted skin friction coefficients fell slightly below the data uncertainty bands. In general, the agreement between the data and predictions was very good. This agreement is in spite of the fact that no empirical inputs from the conical roughness were used to refine the roughness element heat transfer and drag closure models required in the discrete element approach. A geometric description of the roughness element shape and spacing was the only input particular to the conical roughness.

Acknowledgement—This research was supported in part by the U.S. Air Force Office of Scientific Research under Grants AFOSR-85-0075 and AFOSR-86-178. The authors gratefully acknowledge the interest and encouragement of Capt. Hank Helin and Dr James McMichael.

REFERENCES

1. M. H. Hosni, H. W. Coleman and R. P. Taylor, Measurements and calculations of rough-wall heat transfer in the turbulent boundary layer, *Int. J. Heat Mass Transfer* **34,** 1067–1082 (1991).
2. M. H. Hosni, H. W. Coleman and R. P. Taylor, Measurement and calculation of surface roughness effects on turbulent flow and heat transfer, Report TFD-89-1, Mechanical and Nuclear Engineering Department, Mississippi State University (1989).
3. R. P. Taylor, H. W. Coleman and B. K. Hodge, A discrete element prediction approach for turbulent flow over rough surfaces, Report TFD-84-1, Mechanical and Nuclear Engineering Department, Mississippi State University (1984).
4. R. P. Taylor, H. W. Coleman and B. K. Hodge, Prediction of turbulent rough-wall skin friction using a discrete element approach, *J. Fluids Engng* **107,** 251–257 (1985).
5. W. F. Scaggs, R. P. Taylor and H. W. Coleman, Measurement and prediction of rough wall effects on friction factor—uniform roughness results, *J. Fluids Engng* **110,** 385–391 (1988).
6. R. P. Taylor, H. W. Coleman, M. H. Hosni and P. H. Love, Thermal boundary condition effects on heat transfer in the turbulent incompressible flat plate boundary layer, *Int. J. Heat Mass Transfer* **32,** 1165–1174 (1989).
7. J. W. Garner, M. H. Hosni, H. W. Coleman and R. P. Taylor, An investigation of surface roughness shape effects on turbulent flow and heat transfer, Report TFD-90-1, Mechanical and Nuclear Engineering Department, Mississippi State University (1990).
8. W. M. Kays and M. E. Crawford, *Convective Heat and Mass Transfer*, 2nd Edn. McGraw-Hill, New York (1980).